Design, Modelling and Simulation of a Monolithic High-T_c Superconducting Terahertz Mixer

Xiang Gao[1], Ting Zhang[2], Jia Du[1], Yingjie Jay Guo[2]

[1] CSIRO Manufacturing, PO Box 218, Lindfield, NSW 2070, Australia;

[2] Global Big Data Technologies Centre, University of Technology Sydney, Ultimo, NSW 2007, Australia;

Abstract

This paper presents a novel concept and the design of a full monolithic-integrated high-T_c superconducting (HTS) Josephson-junction terahertz (THz) harmonic mixer coupled with a circularly polarized (CP) antenna. The fully on-chip mixer device is very compact in size and utilizes the CP antenna to enhance the polarization orientation flexibility in coupling the THz radiations. Electromagnetic (EM) simulations are carried out to optimize the coupling efficiency and axial ratio of the THz CP antenna, and the signal transmission and isolation characteristics of the monolithic circuit. An equivalent circuit model of the HTS THz mixer is then established and simulation is performed based on our previously measured step-edge Josephson junction characteristics to evaluate the device performance and validate the concept of design. The results show that superior performance could be achieved from such a monolithic HTS mixer device, which is significantly better than any HTS THz harmonic mixers reported to date.

1. Introduction

Ultrahigh bitrate wireless links are increasingly in demand for many practical applications, such as last-mile broadband wireless access, real-time transmissions of high-definition video signals, and fast restoration of network connections after natural disasters [1, 2]. To accommodate the growing needs, the communication carrier frequency has been pushed higher and higher towards sub-millimetre and terahertz (THz) bands. The considerable bandwidth of THz wave brings great benefits to wireless communications, such as overcoming the system capacity bottleneck. However, due to

the limited source power and severe atmospheric attenuation at the THz bands, the receiver system must be very sensitive for reliable signal detection, particularly over longer communication ranges. High-T_c superconducting (HTS) Josephson-junction mixers are promising candidates for THz communication receiver frontends due to their high sensitivity, wide bandwidth, and lower cryogenic cost compared to that for cooling the low-T_c superconducting (LTS) devices. Early demonstrations of HTS THz mixers were mostly achieved in the temperature ranges below 20 K [3-6] and later at 58 K [7]. Recently, HTS THz mixers that operate up to 77 K have been demonstrated at CSIRO laboratory [8-11] using a step-edge junction technology [12]. Best noise and conversion performance at 600 GHz band were achieved [13].

In this paper, we propose a completely new concept of a full monolithic-integrated circularly polarized (CP) antenna-coupled HTS THz harmonic mixer that comprises not only the antenna but all other components including the diplexer and bias-tee on chip. Due to the removal of resistive connection losses between components and better signal coupling design, significant performance improvement is expected from such a design. We shall show in this paper by modelling and simulation that significantly better mixer performance is indeed obtained based on the same Josephson junction parameters as that of the previously measured mixer [9, 10]. To the best of our knowledge, this is the first attempt of designing a full on-chip HTS THz mixer receiver. In addition to achieving the best device performance, such a monolithic integrated mixer configuration is hugely advantageous for constructing a compact cryogenic receiver and implementing a multi-channel architecture as a low cooling power is required. In addition, the novel THz CP antenna greatly enhances polarization orientation flexibility while achieving high-efficiency radiation coupling. This is particularly useful for its application to moving platforms where the polarization orientation constantly varies. Detailed device design, modelling analysis and mixer performance simulation are presented in following sections.

2. On-Chip HTS Mixer Design

Figure 1 shows the schematic of the presented monolithic HTS THz mixer, where the THz CP antenna, diplexer, and bias-tee are integrated with the HTS Josephson junction on a single chip to form a full HTS receiver front-end. Under the harmonic mixing operation mode, the THz signal coupled into the junction via the CP antenna is down-converted into an intermediate-frequency (IF) signal after mixing with a high-order harmonic of a local oscillator (LO) pumping signal at the Ka band (32 to 38 GHz). The on-chip diplexer and bias-tee networks are utilized to achieve good transmission and

isolation of the LO, IF and DC biasing signals. Figure 2(a) shows the design layout of the monolithic mixer device integrated on a piece of 10 × 10 mm^2 MgO substrate with a thickness of 0.5 mm. The THz CP antenna lies in the upper right corner of the mixer chip (see the pink dashed box), and an anti-reflective (AR) Parylene-coated silicon (Si) lens is attached on backside for achieving highly directional radiation. A coplanar waveguide (CPW) diplexer is designed to achieve effective transmission and isolation of the LO and IF signals, which consists of a seventh-order stepped-impedance lowpass filter and a three-order capacitive-gap coupled resonator bandpass filter. A coplanar bias-tee based on a resistor-capacitor (RC) network and high-impedance CPW lines is designed to separate the DC bias and IF signals. Four DC pads are created for applying the four-point method (*I*+, *V*+, *I*-, *V*-) to measure the current-voltage characteristics (IVCs) of the HTS Josephson junction. Bonding ribbons are utilized for those CPW networks to suppress the unwanted coupled-slotline (CSL) mode [14]. Furthermore, considering the junction dynamic resistance value (usually in an order of a few tens of Ω), the diplexer and bias-tee are designed to be matched to 50 Ω.

The presented mixer integrates a novel CP antenna to couple the THz radiations into the HTS Josephson junction with enhanced signal coupling efficiency and polarization orientation flexibility. Figure 2(b) shows the geometry of the designed THz CP antenna including the impedance matching and isolation networks. The main radiator is a modified ring-slot thin-film structure loaded with two perturbed square notches at its diagonal corners. Good CP radiation can be realized by adjusting the notches dimension to handle the magnitude and phase relationships for two orthogonal linearly-polarized (LP) field modes. Two air bridges are used to suppress the excitation of the undesired CSL mode resulting from the asymmetrical discontinuities introduced by notch loading. The HTS Josephson junction is located at the antenna port, and due to its low normal resistance R_n (typical value: 5 Ω), a 50-Ω CPW line transformer is utilized to minimize the impedance mismatch between the junction and the ring-slot antenna. On left side of the slot antenna is a CPW isolation network consisting of a fifth-order stepped-impedance choke filter to prevent the THz electric current from leaking onto the microwave ports.

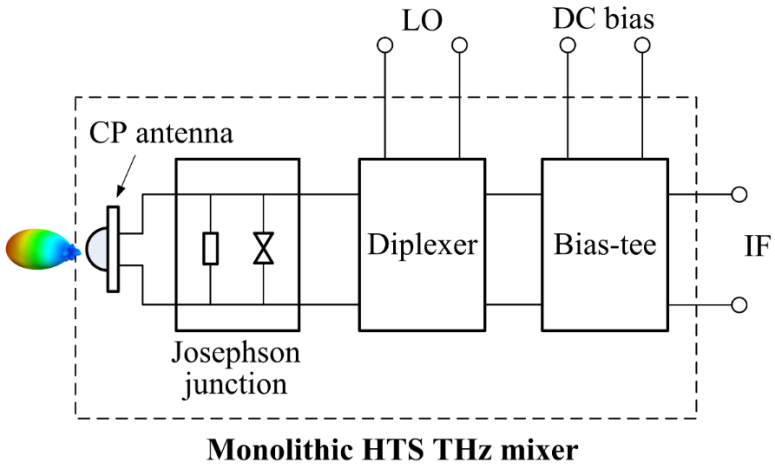

Figure 1. Schematic of the monolithic-integrated CP antenna-coupled HTS Josephson-junction THz harmonic mixer; all components in the dashed line box are integrated on-chip.

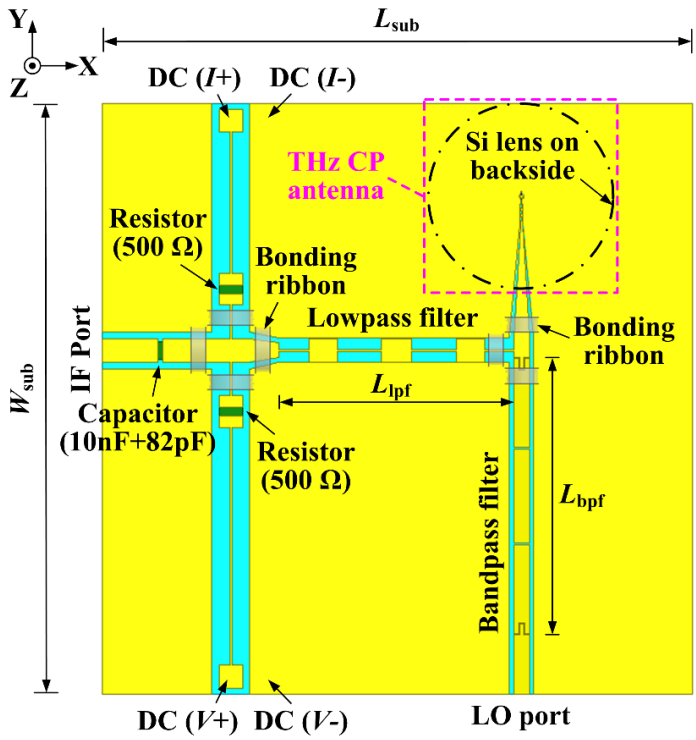

(a)

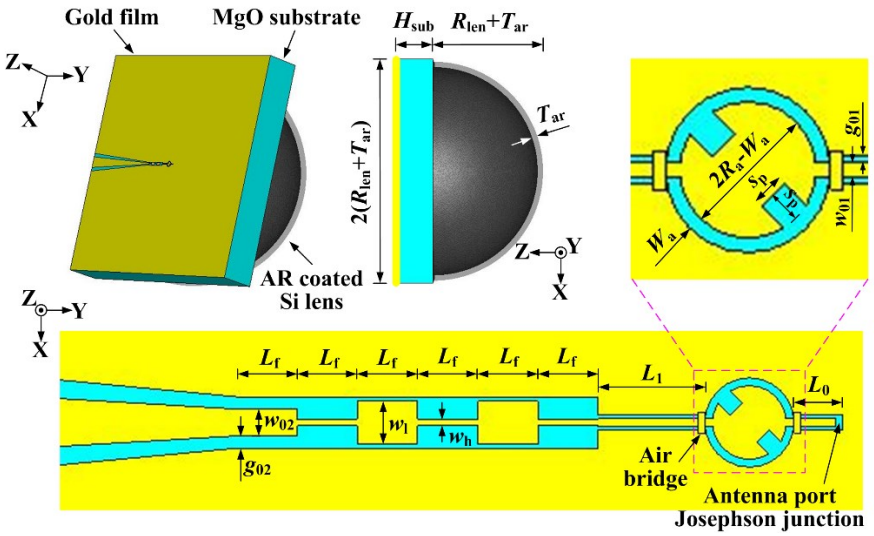

(b)

Figure 2. (a) Design layout of the presented monolithic HTS THz mixer; (b) geometry of the THz CP antenna with a Josephson junction integrated at its port. (Structural parameters: L_{sub} = W_{sub} = 10 mm, H_{sub} = 0.5 mm, R_{len} = 1.5 mm, T_{ar} = 77 μm, L_{lpf} = 3.98 mm, L_{bpf} = 4.69 mm, R_a = 40 μm, W_a = 7 μm, s_p = 16 μm, w_{01} = 7 μm, g_{01} = 3 μm, w_{02} = 24 μm, g_{02} = 11 μm, w_h = 6 μm, w_l = 38 μm, L_f = 54 μm, L_1 = 96 μm, and L_0 = 44 μm.)

3. Electromagnetic Modelling Analysis

After careful design and optimization through electromagnetic (EM) simulations, the final device structural parameters are obtained as shown in the caption of figure 2. Figures 3-7 show the EM analysis results of the monolithic-integrated CP antenna-coupled HTS THz mixer. A coupling efficiency η_c [9] is defined for the antenna to quantify its capability of coupling THz radiation into the HTS Josephson junction. By simulation with the Computer Simulation Technology (CST) software, it is found that as shown in figure 3, the antenna has a high coupling efficiency achieving -3.1 dB at the resonant frequency of 600 GHz, and a 1.5-dB operating bandwidth of 570 to 627 GHz. The good results are attributed to an effective design for minimizing impedance mismatch loss, where the optimized antenna input resistance of 20 Ω at 600 GHz is relatively low, closer to the junction normal resistance (assumed 5 Ω here), than the antennas in earlier work [8-11]. Figure 3 also shows the axial ratio characteristics in the negative Z direction. It is found that the THz antenna exhibits very good CP radiation with the axial ratio less than 3 dB over a frequency band from 572 GHz to 627 GHz. Figure 4 is the simulated radiation pattern of the antenna at 600 GHz, and it shows a highly-

directional left-handed circularly-polarized (LHCP) radiation. The radiation pattern exhibit very good symmetry in the XZ and YZ planes, and the side-lobe and cross-polarization [right-handed circular polarization (RHCP)] levels are all below -15 dB. The LHCP realized gain of the THz antenna is around 20-21 dB over the whole operating frequency band.

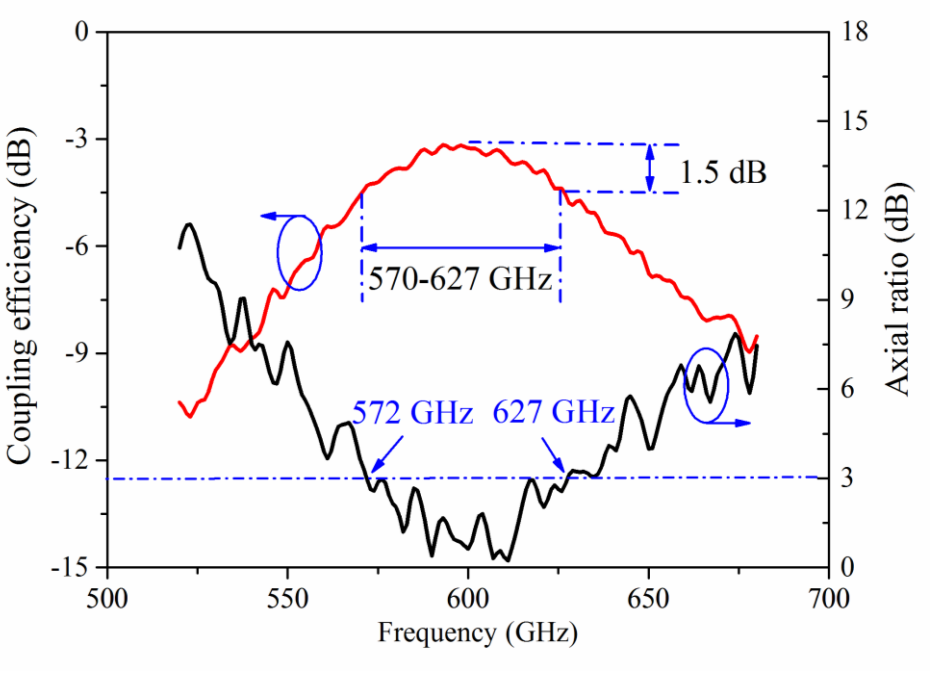

Figure 3. Simulated coupling efficiency and axial ratio of the THz CP antenna.

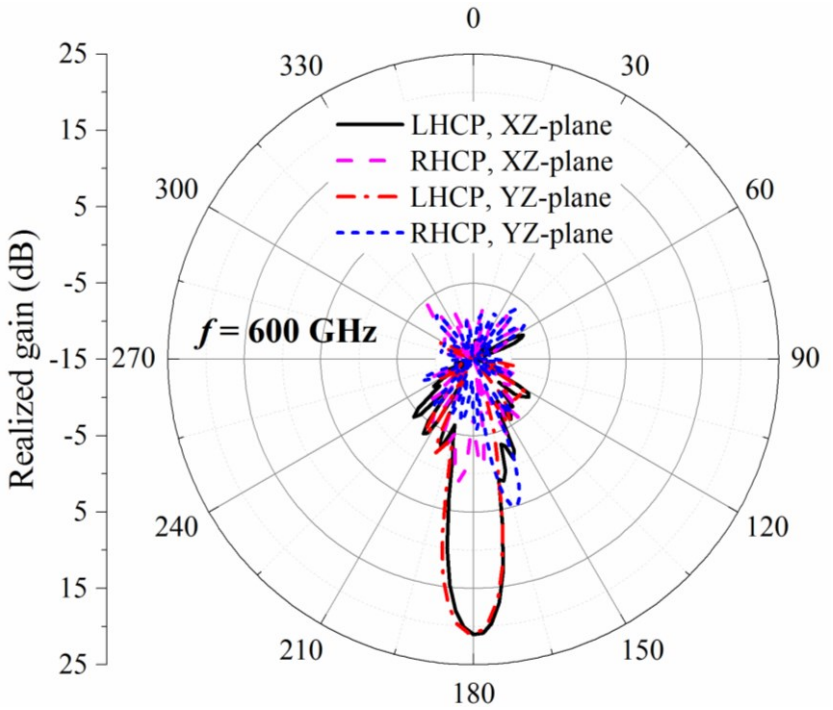

Figure 4. Simulated radiation pattern of the THz CP antenna at 600 GHz.

Figure 5 shows the simulated surface electric current distribution on the THz CP antenna at 600 GHz. Seen from figure 5(a), the THz current has been effectively blocked by the isolation network from leaking to the leftmost end of the CPW line (for microwave signal transmission). Furthermore, a current valley is observed at the right end of the fifth-order stepped-impedance choke filter, which indicates that the left end of the ring-slot antenna can be regarded as a virtual "open" after an approximately half-wavelength CPW line (see "L_1" in figure 2). Consequently, the field modes of the ring-slot antenna would not be influenced by the CPW isolation work. It should be emphasized that although there are some electric currents on the CPW lines, they do not contribute to THz radiations due to the mutual cancellation effect. Figure 5(b) shows the current vector distribution at the phases of 0°, 90°, 180° and 270°, respectively. Obviously, the THz antenna radiates a LHCP wave towards the negative Z direction.

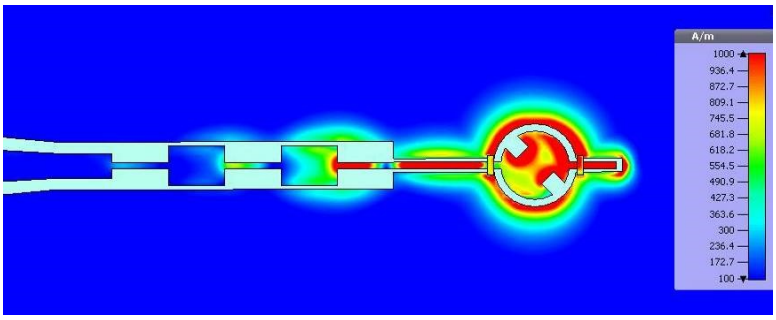

(a)

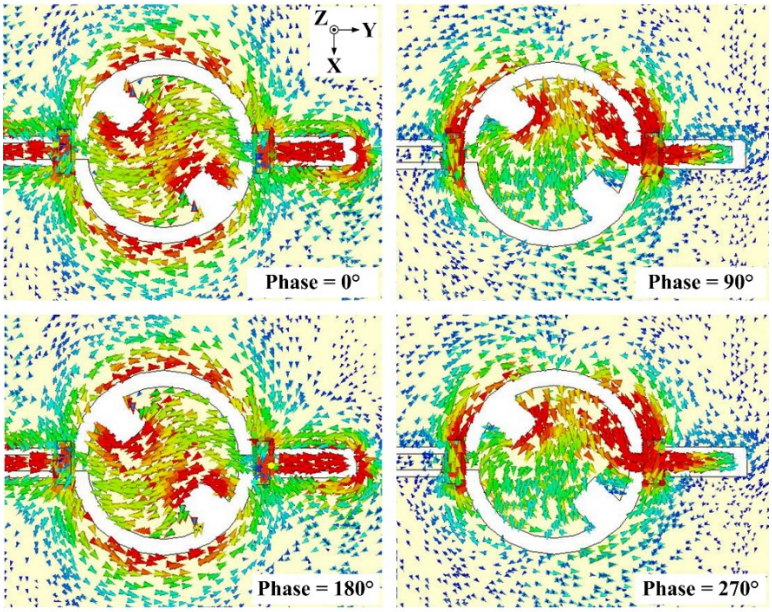

(b)

Figure 5. Simulated surface electric current distribution on the THz CP antenna at 600 GHz: (a) current amplitude; (b) current vector at different phases.

Figure 6 shows the simulated transmission coefficients from the Josephson junction to the LO and IF ports, respectively, which are obtained by using the software High Frequency Structural Simulator (HFSS). Clearly, a bandpass frequency response is observed for the LO signal transmissions, which has a 3-dB passband from 31.2 GHz to 38.8 GHz; a lowpass response with a 3-dB cutoff frequency up to 18 GHz for the IF transmission. Furthermore, the monolithic-integrated circuit exhibits very good port isolation characteristics, achieving more than 20 dB for the LO and 40 dB for the IF signals, respectively. Figure 7 shows the simulated electric current distribution at the frequencies of 35 GHz and 6.5 GHz, which further clarifies the good signal transmission and isolation performance of the monolithic HTS THz mixer.

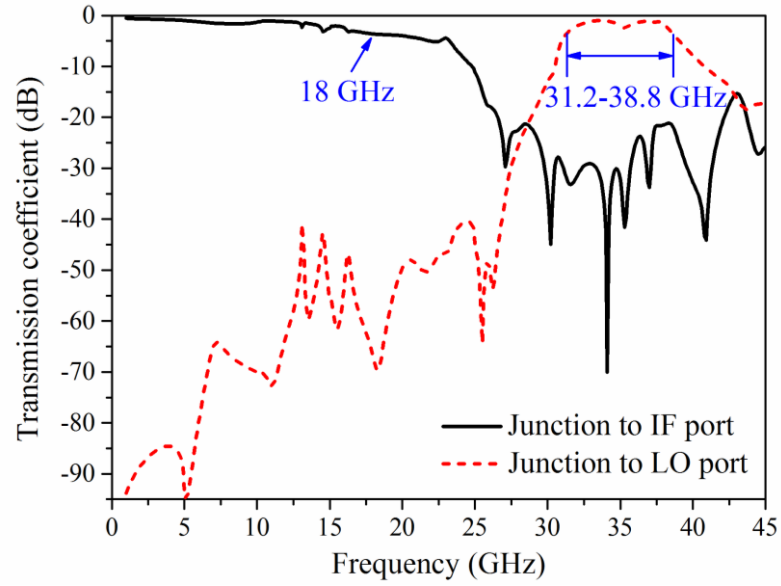

Figure 6. Simulated transmission coefficients from the Josephson junction to the LO and IF ports.

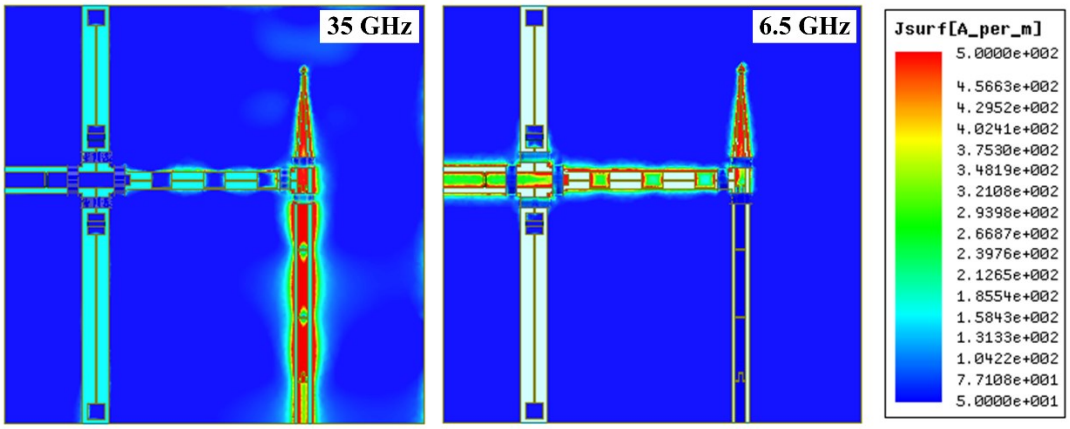

Figure 7. Simulated electric current distribution on the monolithic-integrated circuit at the frequencies of 35 GHz (LO) and 6.5 GHz (IF).

4. HTS Josephson-Junction Mixer Simulation and Discussion

With the aim of validating the concept of design, active device modelling (after passive EM simulation) is carried out to evaluate the frequency conversion performance of the monolithic HTS THz mixer. The simulation method was recently developed by our group and has been described in details in [15]. The method combines the software Keysight Advanced Design System (ADS) with an imported Verilog-A model of the Josephson junction to model the full HTS monolithic microwave integrated circuit (MMIC) mixer, which has been successfully applied for modelling a Ka-band HTS MMIC receiver earlier [16]. Considering its powerful capability and high accuracy in analyzing the HTS Josephson devices that contain complicated peripheral networks (e.g. the matching and filter circuits), we have applied this approach to model the monolithic-integrated CP antenna-coupled HTS THz harmonic mixer presented in this paper.

Based on the EM analysis results described above, an equivalent circuit model is established for the HTS THz mixer device as shown in figure 8. The current biasing, RF, LO and IF links are connected in parallel with the resistively-shunted HTS Josephson junction. A bandpass filter BPF_1 is used to describe the antenna performance in coupling THz radiations, which has an insertion loss of 3.1 dB at the central frequency of 600 GHz and a 1.5-dB passband bandwidth of 570 to 627 GHz. The left side of BPF_1 is matched to the junction normal resistance R_n and right side matched to the RF source impedance Z_{RF} (i.e., the free-space wave-impedance). Another bandpass filter BPF_2 (with a 3-dB passband from 31.2 GHz to 38.8 GHz) is introduced between the LO source and the Josephson junction, which features insertion losses of 1.5 dB at 35 GHz and 40 dB at 26.8 GHz, respectively. In addition, a lowpass filter LPF (3-dB passband: 0 to 18 GHz) is utilized to describe the IF transmission characteristics, which has insertion losses of 0.5 dB at 1 GHz and 32 dB at 35 GHz, respectively. Both sides of BPF2 and LPF are matched to 50 Ω. A Capacitor is included to prevent the bias current from leaking into the IF link. The DC, THz, LO and IF signals are well isolated from each other through these equivalent filters and capacitors.

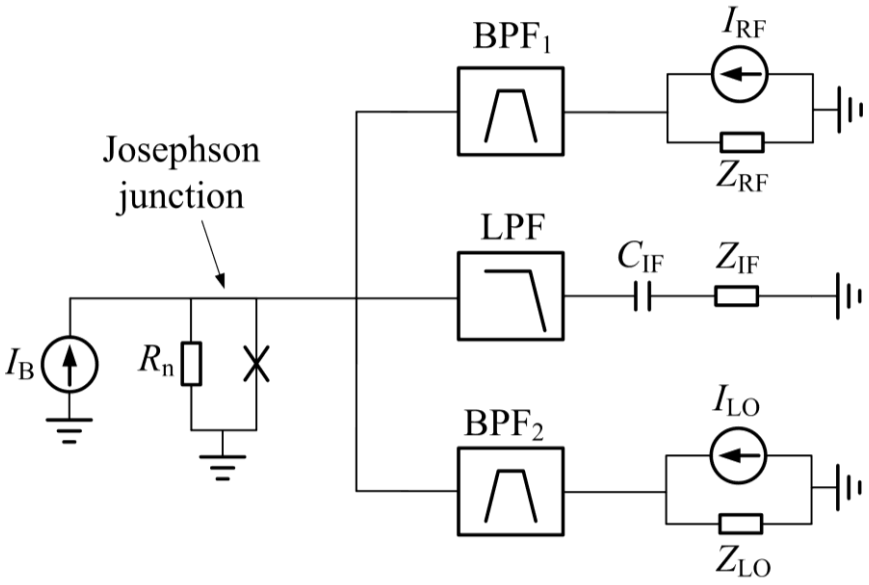

Figure 8. Equivalent circuit model of the presented monolithic HTS THz mixer device (R_n = 5 Ω, Z_{RF} = 377 Ω, $Z_{LO} = Z_{IF}$ = 50 Ω, C_{IF} = 10.082 nF).

Although the circuit design and modelling are applicable for different types of HTS Josephson junctions, the mixer device simulation here will be based on our step-edge junction characteristics. Figure 9 shows the simulated DC IVCs of the presented HTS THz mixer (assume T = 40 K, where the junction characteristics were extensively measured in previous work [9, 10]). Clearly, the unpumped HTS Josephson junction exhibits a typical resistively-shunted-junction (RSJ) behaviour (see black curves). Under the THz illumination or LO pumping, the junction critical current I_c is partly suppressed and the suppression increases with increasing the source current I_{RF} or I_{LO}. Moreover, there are a series of Shapiro steps induced in the pumped I-V curves shown in figure 9(a). As predicted by the Josephson voltage-frequency equation [17]: $V_n = n\Phi_0 f_{RF}$ (where n is an integer, Φ_0 is the magnetic flux quantum, and f_{RF} is the signal frequency), the voltage of the first induced Shapiro step is located exactly at 1.24 mV for the THz pumping at 600 GHz. The Shapiro steps induced by LO pumping are less visible in figure 9(b) due to a much lower frequency (36.9375 GHz) thus small steps in a large voltage scale. In the simulation, the Josephson junction parameters (R_n = 5 Ω and unpumped I_c = 310 μA) are extracted from the measured results of the previous mixer described in reference [10]. Using the same junction characteristics can provide a fair comparison of mixing performance between this new design and previous devices. The I_c and R_n values are typical ones for our developed HTS step-edge junctions operating at 40 K.

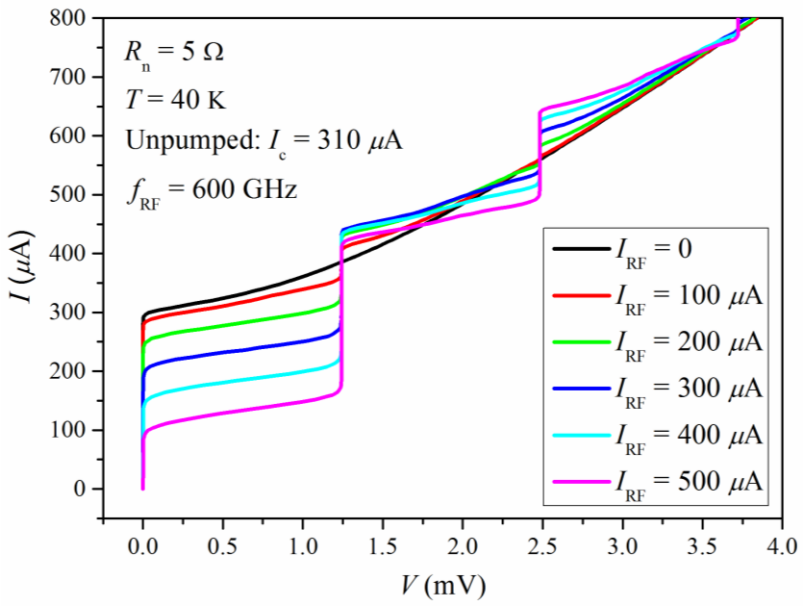

(a)

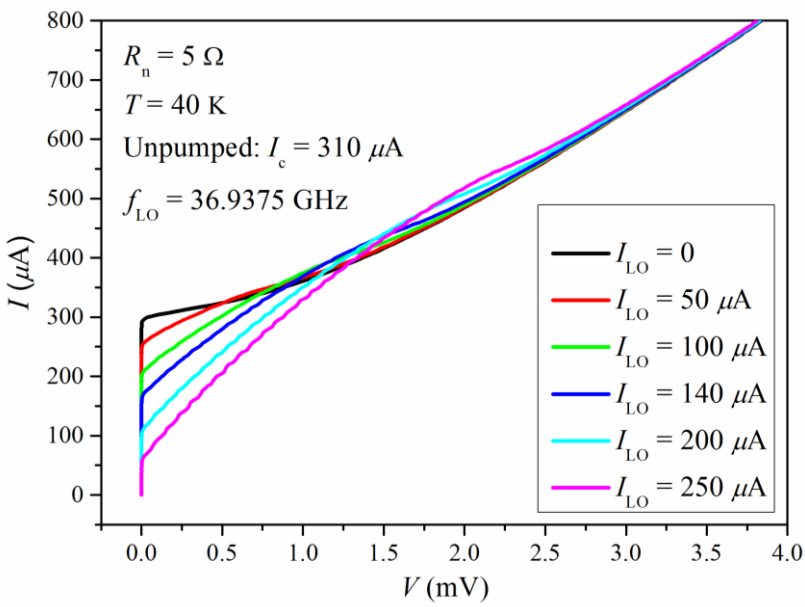

(b)

Figure 9. Simulated DC IVCs of the Josephson junction under the (a) THz illumination and (b) LO pumping.

Figures 10-12 show the simulated frequency down-conversion performance of the monolithic HTS THz mixer at temperature of 40 K. A 600-GHz THz signal is down-converted to a 5.4-GHz IF signal when mixing with the 16th harmonic of a LO pumping signal at 36.9375 GHz. Figure 10 shows the simulated relationship of the IF output power P_{IF} versus THz input power P_{RF}, where the mixer

exhibits good linearity at a lower P_{RF} range and then tends to saturate when P_{RF} is increased to near the LO power P_{LO}. The maximum mixer conversion gain G_{mix} (i.e., P_{IF} / P_{RF}) is about -33 dB and the 1-dB gain compression point is at P_{RF} = -53 dBm.

Figure 11 shows the bias current (I_B) dependence of the mixer conversion gain. The G_{mix} versus I_B relationship exhibits a strong modulation phenomenon with a number of resonant peaks appear. This has been observed in previous experiment [8] and is believed to be resulted from the Shapiro steps induced by LO pumping; the P_{IF} minima occur at integer multiples or harmonics of the LO frequency f_{LO}, although might not at every value [11]. Furthermore, it is found from figure 11 that the mixer has a relatively wide bias current range (more than 200 μA at P_{LO} = -35 dBm) which further increases as the LO power rises.

Figure 12 shows the simulated frequency response of the mixer at the 600-GHz band. Under the 16th harmonic mixing at optimal I_B and P_{LO}, the mixer conversion gain is around -32.5 dB over a wide operating bandwidth of 592 to 611 GHz for RF and 1 to 20 GHz for IF, respectively. The minor fluctuation in the frequency response trace mainly results from a slight mismatch between the junction dynamic resistance and the input impedance of the IF lowpass filter (matched to 50 Ω).

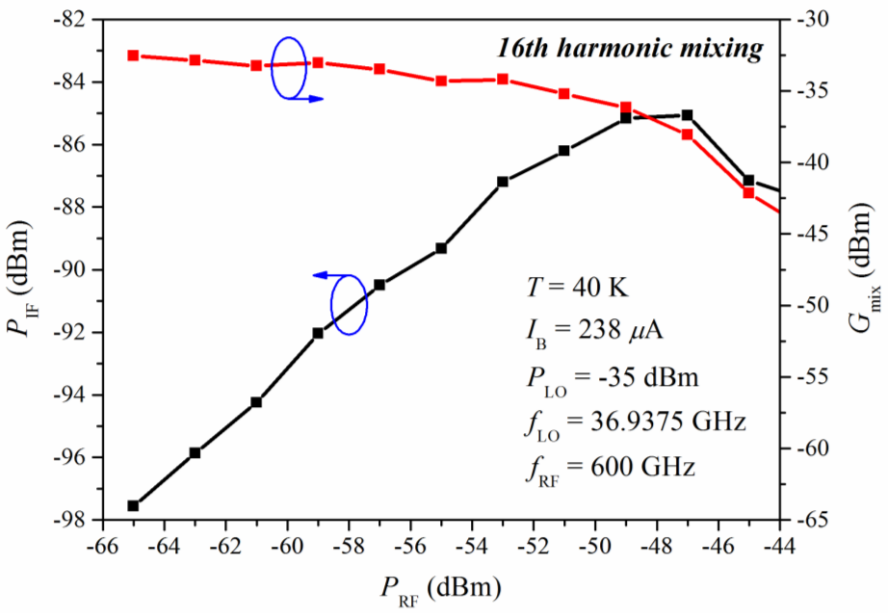

Figure 10. Simulated IF output power P_{IF} and mixer conversion gain G_{mix} versus the THz input power P_{RF}.

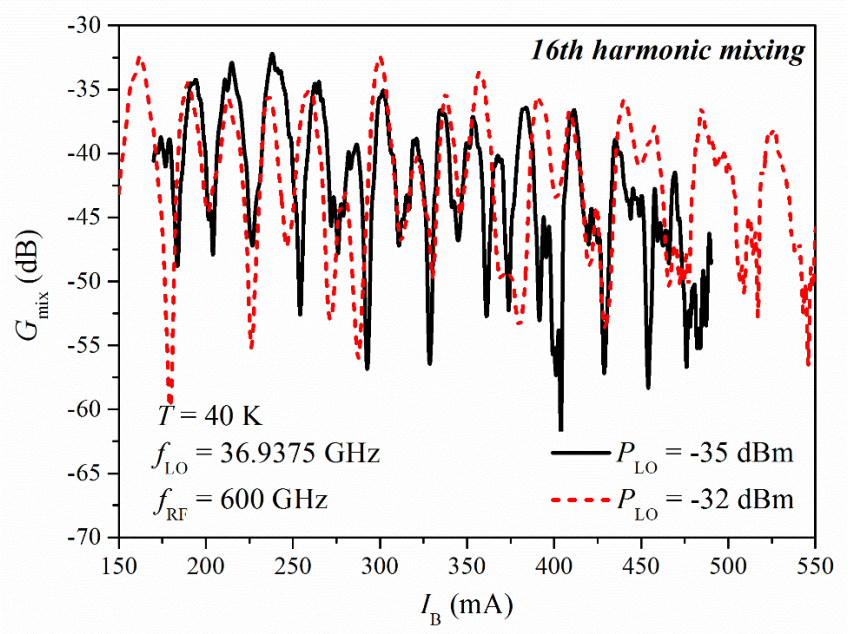

Figure 11. Simulated mixer conversion gain G_{mix} versus the bias current I_B for different LO pumping power P_{LO}.

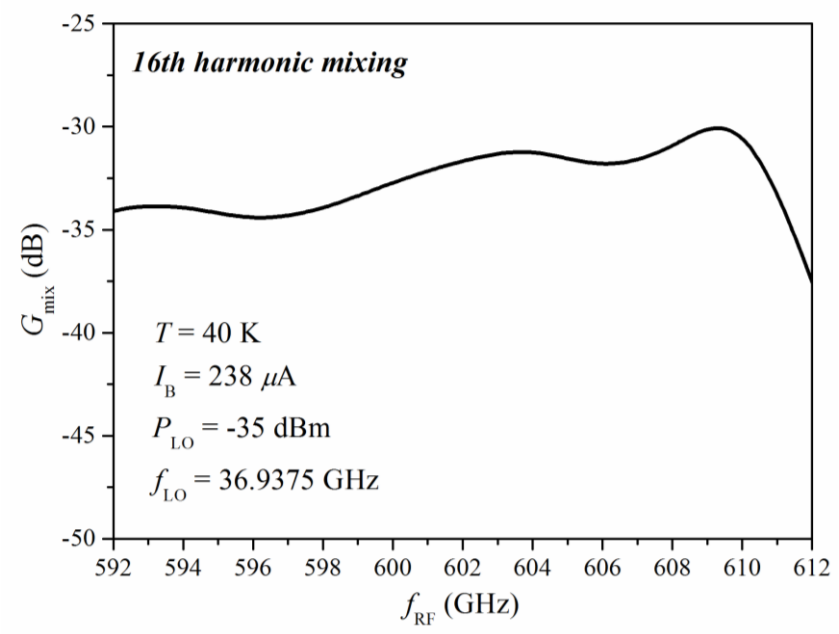

Figure 12. Simulated frequency response of the HTS THz mixer.

The achieved mixer conversion gain is around 17 dB higher than the best reported results [8, 10] to date for HTS THz harmonic mixers at the comparable frequencies and operating temperatures. The current design of full on-chip circuit plus the new THz CP antenna results in a significant performance

improvement from our previous mixer results [10] assuming the same Josephson junction characteristics. Such a large improvement is mainly due to the removal of resistive connection losses between components, better signal coupling designs, and efficient signal isolation circuit for the RF, LO, and IF ports. The simulation results have validated that the all-inclusive monolithic HTS circuit at THz band is an innovative design that brings major performance improvement desired for sensitive THz wireless receiver systems.

5. Conclusion

A novel monolithic-integrated CP antenna-coupled HTS Josephson-junction THz harmonic mixer is presented in this paper. The mixer has a compact feature that all its relevant components are integrated on a single 10 × 10 mm^2 chip, which provides more efficient signal coupling thus low loss and exhibits enhanced polarization orientation flexibility in coupling THz radiations. Full device design, modelling analysis and performance evaluation are provided in detail. Superior performance is demonstrated, that is an increase of around 17 dB in conversion gain compared to our previously demonstrated HTS mixer of identical Josephson junction characteristics. Such a new concept of monolithic HTS THz mixer will have huge potential for ultra-sensitive and ultrahigh-bitrate THz wireless applications.

References

1. Schneider T 2014 Ultrahigh-bitrate wireless data communications via THz-links; possibilities and challenges *J. Infrared Millimeter THz Waves* **36** 159-179.

2. Ducournau G, Szriftgister P, Pavanello F, Peytavit E, Zaknoune M, Bacquet D, Beck A, Akalin T, Lampin J-F and Lampin J-F 2015 THz communications using photonics and electronic devices: the race to data-rate *J. Infrared Millimeter THz Waves* **36** 198-220.

3. Chen J, Myoren H, Nakajima K, Yamashita T and Wu P H 1997 Mixing at terahertz frequency band using $YBa_2Cu_3O_{7-\delta}$ bicrystal Josephson junctions *Appl. Phys. Lett.* **71** 707-709.

4. Shimakage H, Uzawa Y, Tonouchi M and Wang Z 1997 Noise temperature measurement of YBCO Josephson mixers in millimetre and submillimeter waves *IEEE Trans. Appl. Supercond.* **7** 2595-2598.

5. Harnack O, Darula M, Scherbel J, Heinsohn J-K, Siegel M, Diehl D and Zimmermann P 1999 Optimization of a 115 GHz waveguide mixer based on an HTS Josephson junction *Supercond. Sci. Technol.* **12** 847-849.

6. Scherbel J, Darula M, Harnack O and Siegel M 2002 Noise properties of HTS Josephson mixers at 345 GHz and operating temperatures at 20 K *IEEE Trans. Appl. Supercond.* **12** 1828-1831.

7. Malnou M, Feuillet-Palma C, Ulysse C, Faini G, Febvre P, Sirena M, Olanier L, Lesueur J and Bergeal N 2014 High-T_c superconducting Josephson mixers for terahertz heterodyne detection *J. Appl. Phys.* **116** 074505.

8. Du J, Weily A R, Gao X, Zhang T, Foley C P and Guo Y J 2016 HTS step-edge Josephson junction terahertz harmonic mixer *Supercond. Sci. Technol.* **30** 024002.

9. Gao X, Zhang T, Du J, Weily A R, Guo Y J and C P Foley 2017 A wideband terahertz high-T_c superconducting Josephson-junction mixer: electromagnetic design, analysis and characterization *Supercond. Sci. Technol.* **30** 095011.

10. Gao X, Du J, Zhang T, Guo Y J and Foley C P 2017 Experimental investigation of a broadband high-temperature superconducting terahertz mixer operating at temperatures between 40 and 77 K *J. Infrared Millimeter THz Waves* **38** 1357-1367.

11. Du J, Pegrum C, Gao X, Weily A R, Zhang T, Guo Y J and Foley C P 2017 Harmonic mixing using a HTS step-edge Josephson junction at 0.6 THz frequency *IEEE Trans. Appl. Supercond.* **27** 1500905.

12. Foley C P, Mitchell E E, Lam S K H, Sankrithyan B, Wilson Y M, Tilbrook D L and Morris S J 1999 Fabrication and characterisation of YBCO single grain boundary step edge junctions *IEEE Trans. Appl. Supercond.* **9** 4281-4284.

13. Gao X, Du J, Zhang T and Guo Y J 2017 Noise and conversion performance of a high-T_c superconducting Josephson junction mixer at 0.6 THz *Appl. Phys. Lett.* **111** 192603.

14. Lee J, Lee H, Kim W, Lee J and Kim J 1999 Suppression of coupled-slotline mode on CPW using air-bridges measured by picosecond photoconductive sampling *IEEE Microw. Guided Wave Lett.* **9** 265-267.

15. Zhang T, Pegrum C, Du J and Guo Y J 2016 Simulation and measurement of a Ka-band HTS MMIC Josephson junction mixer *Supercond. Sci. Technol.* **30** 015008.

16. Zhang T, Gao X, Wang W, Du J, Pegrum C, Guo Y J 2017 A 36 GHz HTS MMIC Josephson Mixer - simulation and measurement *IEEE Trans. Appl. Supercond.* **27** 1502405.

17. Duzer T V and Turner C W 1999 *Principles of Superconductive Devices and Circuits* (Upper Saddle River, NJ, USA: Prentice-Hall).